

# Multi-Agent Reinforcement Learning–Based UAV Pathfinding for Obstacle Avoidance in Stochastic Environment

Qizhen Wu, Kexin Liu, Lei Chen, *Member, IEEE*, and Jinhu Lü, *Fellow, IEEE*

**Abstract**—Traditional methods plan feasible paths for multiple agents in the stochastic environment. However, the methods’ iterations with the changes in the environment result in computation complexities, especially for the decentralized agents without a centralized planner. Although reinforcement learning provides a plausible solution because of the generalization for different environments, it struggles with enormous agent–environment interactions in training. Here, we propose a novel centralized training with decentralized execution method based on multi-agent reinforcement learning, which is improved based on the idea of model predictive control. In our approach, agents communicate only with the centralized planner to make decentralized decisions online in the stochastic environment. Furthermore, considering the communication constraint with the centralized planner, each agent plans feasible paths through the extended observation, which combines information on neighboring agents based on the distance–weighted mean field approach. Inspired by the rolling optimization approach of model predictive control, we conduct multi-step value convergence in multi-agent reinforcement learning to enhance the training efficiency, which reduces the expensive interactions in convergence. Experiment results in both comparison, ablation, and real-robot studies validate the effectiveness and generalization performance of our method.

**Index Terms**—Multi-agent systems, pathfinding, deep reinforcement learning, unmanned aerial vehicle, artificial intelligence.

## I. INTRODUCTION

WITH the development of artificial intelligence, the applications in multi-agent systems [1], [2] are attracting more attention. Pathfinding is a crucial problem in multi-agent systems, where a team of cooperative agents computes collision-free movement plans. In obstacle avoidance problems [3], unmanned aerial vehicles (UAVs) should avoid obstacles and collisions with their neighbors in three dimensions. The uncertain changes of the stochastic environment in obstacle avoidance [4] bring significant challenges to traditional multi-agent pathfinding (MAPF) approaches including graph

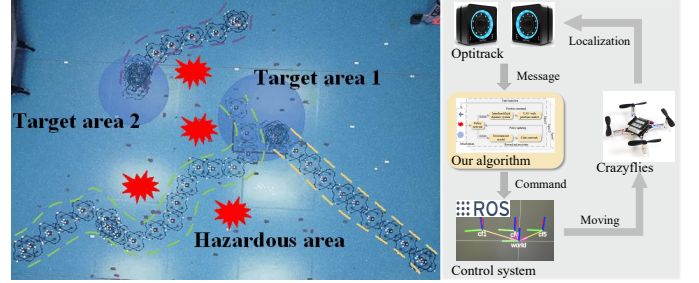


Figure 1. Multi-UAV flight in an uncertain scenario. The blue and red spheres indicate target and hazardous areas, respectively. We consider the multi-UAV obstacle avoidance problem in the scenario where hazardous areas’ locations and numbers are randomly changing at regular intervals. UAVs perform real-time path planning based on the trained policies. In experiments, we maneuver Crazyflies through the ground control center with motion capture from Optitrack.

search [5] and heuristic algorithms [6]. To plan safe paths for agents, the algorithms raise considerable computational efforts in solving these changes, such as randomly appearing hazardous areas generated by explosions or bad weather conditions [7].

Reinforcement learning (RL)–based MAPF algorithms show great potential in solving obstacle avoidance problems in the stochastic environment. As the number of agents grows, multi-agent reinforcement learning (MARL) reduces the computational efforts in obstacle avoidance compared to traditional algorithms. It adopts an end-to-end framework to approach the optimal decision [8], [9], which has the generalization performance for different environments. The MAPF algorithms based on MARL can be categorized by three types: fully centralized, fully decentralized, and centralized training with decentralized execution (CTDE). The fully centralized approach [10] treats multiple agents as a whole system and trains the strategies of all agents through a centralized planner. Under this approach, agents are only able to follow the command of the planner and cannot perform tasks independently. Therefore, it cannot be generalized directly when facing larger-size scenarios and encounters the dimensional explosion problem. In contrast, the fully decentralized method [11] emphasize the independent learning of agents, but ignores the intrinsic influence between each agent, resulting in unstable training. Therefore, problems with the above methods lead to their inability to be applied further in large-scale MAPF.

To emerge coordination behaviors among fully decentralized agents, Damani et al. [12] combine MARL with imitation

\*This work was supported in part by the National Key Research and Development Program of China under Grant 2022YFB3305600, and in part by the National Natural Science Foundation of China under Grants 62141604, 62088101, and 62003015. (Corresponding author: Lei Chen.)

Qizhen Wu, Kexin Liu, and Jinhu Lü are with the School of Automation Science and Electrical Engineering, Beihang University, Beijing 100191, China. (e-mail: wuqzh7@buaa.edu.cn; skxliu@163.com; jhlu@iss.ac.cn)

Lei Chen is with the Advanced Research Institute of Multidisciplinary Sciences and State Key Laboratory of CNS/ATM, Beijing Institute of Technology, Beijing 100081, China. (e-mail: bit\_chen@bit.edu.cn)

The experiment video is available at [https://www.bilibili.com/video/BV1gw41197hV/?vd\\_source=9de61aeedd9fb684e546d032ef7fe7bf](https://www.bilibili.com/video/BV1gw41197hV/?vd_source=9de61aeedd9fb684e546d032ef7fe7bf).

The code is available at [https://github.com/Wu-duanduan/CTFDE\\_MPC](https://github.com/Wu-duanduan/CTFDE_MPC).

learning and train the agents with an expert centralized planner. However, the dependence on expert experience limits its scalability to complex tasks. Due to the increasing need for scalability and convergence of algorithms, CTDE learns cooperative strategies in training by sharing information among agents while guaranteeing decentralized decision-making in execution. Recent works [13], [14] apply CTDE to a static-obstacle avoidance scenario, where agents only utilize local and relative information to plan paths distributively, however, it can not generalize to the stochastic environment existing dynamic obstacles. Hence, faced with the stochastic environment with uncertain changes, Guan et al. [15] combine CTDE with the attention mechanism, which allows each agent to consider the behaviors of its surroundings. Moreover, Wang et al. design a mean field-based MARL method for agents to combine information on their surroundings equally. Although the above methods achieve favorable results in simulations, they are difficult to apply directly to real-robot systems because of the extensive agent-environment interactions required during training.

Here, we present a novel CTDE method improved by model predictive control (MPC) for solving obstacle avoidance problems in the stochastic environment. Firstly, we propose a centralized training with partially decentralized execution (CTPDE) method to plan feasible and safe paths for UAVs in uncertain scenarios. Secondly, considering the communication constraint with the centralized planner, we present a centralized training with fully decentralized execution (CTFDE) method, where UAVs can make fully decentralized decisions through extended observations. The method quantifies the varying strengths of interactions among UAVs based on the distance-weighted mean field approach, which enables UAVs to combine information on their neighbors efficiently. Thirdly, inspired by the rolling optimization approach of MPC, we adopt an improved MARL method conducting multi-step value convergence to reduce agent-environment interactions. Finally, experiments in our settings verify that our approach outperforms the baselines including the non-learning approach and decentralized RL, and they also demonstrate the necessity of the improved MARL method through ablation studies. Plus, our method shows its favorable generalization in various-scale instances and its adaptability to real-robot systems. The main contributions of this paper are summarized as follows.

- We explore that overcoming the communication constraint with the centralized planner is a significant challenge for UAV pathfinding in the stochastic environment, so it is necessary to adopt a distance-weighted mean field approach for UAVs to combine information on their neighbors efficiently.
- Since traditional MARL methods may struggle with massive agent-environment interactions in training, we improve MARL by performing multi-step value convergence and calculating the prediction step with an adaptive truncation approach, which effectively reduces the expensive interactions in convergence.
- Conducting extensive experiments including comparison, ablation, and generalization studies, we verify that our

method outperforms conventional baselines in solution quality and computation efficiency. Moreover, the model trained by our method can be deployed directly to real-robot systems.

We organize the rest of the paper as follows. Section II introduces the research related to our study. Section III provides the preliminaries on MARL and presents the formulation of our problem. Section IV offers a detailed description and implementation of the improved MARL method. Section V describes the experiments of our method. Finally, Section VI presents our conclusions.

## II. RELATED WORKS

### A. Mean Field in Reinforcement Learning

Existing MARL methods are usually limited to a small number of agents. When the number of agents increases significantly, training becomes intractable due to dimensional explosion and exponential growth of agent-agent interactions. To overcome these challenges, Yang et al. [16] propose the mean field approach, which replaces the effects produced by neighbors on the individual agent adopting mean values. As a result, the method reduces the interactions between an agent and its neighbors to the interaction between the two agents. It greatly simplifies the increase in observation space brought about by the number of agents, and the strategies' training is mutually facilitated among agents. The mean field-based MARL methods have been widely applied in scenarios with extensive agents, like edge computing [17], swarm confrontation [18], and UAV pathfinding [19]. However, this approximation weights the interactions among all agents equally, but ignores the different strengths of these interactions, losing accuracy in modeling the complex relationships among agents. Here, we design a distance-weighted mean field method to quantify the varying strengths of agent-agent interactions and establish extended observations for UAVs to combine information on their neighbors efficiently.

### B. Model Exploitation in Reinforcement Learning

To enhance the training efficiency and reduce the agent-environment interactions in convergence, the model-based reinforcement learning (MBRL) method has been extensively discussed. Based on the data-driven technique, the method establishes a virtual environment model to approximate the behaviors, characteristics, and relationships of the interactions between the environment and the agent. The model generates additional interaction data by predicting the state transition and reward based on the agent's state and action, which accelerates the learning process. Dyna [20], as a typical MBRL method, employs a forward dynamic model to predict one-step transition and reward. These virtual data can be leveraged to update the value function facilitating the improvement of training efficiency. The method prefers to construct the virtual model adopting a probabilistic ensemble neural network, which can quantify the aleatoric and epistemic uncertainty in the model [21]. Therefore, several Dyna-style methods perform multi-step rollouts based on the interactions with the ensemble network, like model-based policy optimization

[22]. In addition, the model-based value expansion method [23] conducts multi-step prediction to estimate the future transitions in TD-target, which reduces the estimation error for the value function. Moreover, other methods construct a differentiable model, which produces gradients directly to optimize the policy function, such as imagined value gradients [24]. Inspired by the model-based value expansion method, in prior work [25], we propose a single-agent RL method improved by the multi-step value convergence approach. This study further prompts the model-based approach to be applied in MARL and proposes an adaptive prediction step  $N$  via a truncation method.

### III. PRELIMINARIES AND PROBLEM FORMULATION

#### A. Decentralized Partially Observable Markov Decision Processes

Let  $\mathbb{R}$  denote the set of real numbers.  $\mathbb{E}$  denotes the mathematical expectation. A fully cooperative MARL task can be described in terms of a decentralized partially observable Markov Decision Process (Dec-POMDP) [26]. We represent a Markov game for  $I$  agents as an eight-tuple  $(I, S, Z, A, P, R, O, \gamma)$ , where  $s \in S$  denotes the state of the environment.  $z^i \in Z$  denotes the observation of each agent.  $z = [z^1, \dots, z^I]$  denotes the set of the joint observations of all agents.  $a^i \in A$  and  $a = [a^1, \dots, a^I]$  denote the action of each agent and the set of the joint actions of all agents, respectively.  $P(s, a) : S \times A \times S \rightarrow [0, 1]$  denotes the state transition probabilities that takes place from state  $s_t$  to  $s_{t+1}$  under joint actions  $a$ .  $R(z, a) : Z \times A \rightarrow \mathbb{R}$  denotes the reward function.  $\gamma \in (0, 1)$  denotes the discount factor. We define the observation transition probabilities  $O(z, a) : Z \times A \times Z \rightarrow [0, 1]$  that takes place from joint observations  $z_t$  to  $z_{t+1}$  under joint actions  $a$ . The purpose of each agent is to optimize the policy  $\pi^i$  such that the cumulative rewards  $\sum_{t=1}^{\infty} \gamma^t r_t, r_t \sim R^i$  are maximized under the policy.  $\Gamma^i = (z_0^i, a_0^i, z_1^i, a_1^i, \dots)$  is the trajectory of each agent interacting with the environment under a specific strategy.

#### B. Multi-Agent Deep Deterministic Policy Gradient

The value-based RL estimates the optimal state-action value function  $Q^{i*} : O \times A \rightarrow \mathbb{R}$  through a parameterized neural network  $Q_{\omega}^i(z_t, a_t) \approx Q^{i*}(z_t, a_t) = \mathbb{E}[R^i(z_t, a_t) + \gamma \max_{a'} Q^{i*}(z_{t+1}, a_{t+1})]$ , where  $z_{t+1}, a_{t+1}$  are the observation and action at the following step, respectively. The subscript  $\omega = [\omega^1, \dots, \omega^I]$  is the weighting factor of the value-function network. For  $\gamma \approx 1$ ,  $Q^*$  estimates the discounted return of the optimal strategy over an infinite range. Multi-agent deep deterministic policy gradient (MADDPG) provides the individual value-function network  $Q_{\omega}^i(z_t, a_t)$  for each UAV, which produces the gradients to optimize the policy.  $Q_{\omega}^i(z_t, a_t)$  is a centralized action-value function that takes as input joint actions  $a$ , in addition to joint observations  $z$ , and outputs the Q-value for agent  $i$ .  $Q^{i*}$  can be approximated by an iteratively fitting  $Q_{\omega}^i$  and the loss function is described as

$$L_{\omega}^i = \mathbb{E}_{(z_t, a_t) \sim \mathcal{B}} \|Q_{\omega}^i(z_t, a_t) - y^i\|^2, \quad (1)$$

where  $y^i = R^i(z_t, a_t) + \gamma \max_{a'} Q_{\omega}^i(z_{t+1}, a_{t+1})$  is the Q-target.  $\|\cdot\|$  denotes the Euclidean norm. The subscript  $\omega^-$  is a slow-moving online average. It is updated with the rule  $\omega_{k+1}^- \leftarrow (1 - \zeta) \omega_k^- + \zeta \omega_k$  at each iteration using a constant factor  $\zeta \in [0, 1)$ .  $\mathcal{B}$  is a replay buffer that iteratively grows as data are updated. In addition, MADDPG provides the individual policy network  $\pi_{\beta}^i(z_t^i)$  for each UAV, which allows each agent to compute an action value based on its local observation  $z^i$  during execution. The subscript  $\beta = [\beta^1, \dots, \beta^I]$  is the weighting factor of the policy network and the loss function is denoted as

$$L_{\beta}^i = -\mathbb{E}_{(z_t, a_t) \sim \mathcal{B}} [Q_{\omega}^i(z_t, a_t)]. \quad (2)$$

#### C. Multi-UAV Pathfinding for Obstacle Avoidance

This study considers the multi-UAV pathfinding problem in a stochastic environment where hazardous areas appear randomly. The UAVs should reach the set target areas while avoiding hazardous areas and collisions with neighboring UAVs. The final goal of the task is for all UAVs to reach their target areas. The hazardous areas' locations and numbers are randomly changing at regular intervals. It is worth noting that the randomly appearing hazardous areas will not encompass UAVs. Consider the obstacle avoidance problem with  $I$  UAVs and  $K$  hazardous areas. Let position and velocity vectors in three dimensions be denoted by  $p$  and  $v$ , respectively. If the distance between UAV  $i$  and UAV  $j$  is smaller than the fixed distance threshold  $d_{\text{nei}}$ , we consider that UAV  $j$  is the neighbor of UAV  $i$ , which can be described as  $\forall j \in \mathcal{N}^i, \|p^i - p^j\| < d_{\text{nei}}$ . Similarly, neighboring hazardous area  $k$  should satisfy  $\forall k \in \mathcal{N}^i, \|p^i - p^k\| < d_{\text{nei}}$ , where  $\mathcal{N}^i$  denotes the set of UAV  $i$ 's neighbors. We consider UAVs and hazardous areas as the orb models with radius  $\rho_u$  and  $\rho_o$ , respectively. In addition, the planned UAV three-dimensional path usually needs to satisfy some basic constraints, including the path segment length, flight altitude, and total path length. The three-dimensional path constraints of the UAV in each fixed sampling time  $\Delta T$  can be expressed as follows.

The path segment length constraint refers to the shortest range that the UAV can fly in the direction of the current path before it changes the flight attitude, which can be denoted as

$$Le_t = \sqrt{\|p_t - p_{t-1}\|^2}, \quad (3)$$

where  $Le_t \geq Le_{\min}$  and  $Le_{\min}$  is the minimum path segment length. With this constraint, the UAV can avoid circuitous travel or frequent turns. Considering that the UAV may need to communicate with the centralized planner, we set the following flight height constraint:

$$h_{\min} \leq p_{z,t} \leq h_{\max}, \quad (4)$$

where  $p_{z,t}$  denotes the height in three-dimensional space.  $h_{\max}, h_{\min}$  are the maximum and minimum heights, respectively. The total path length constraint, which means the total path length of the UAV is affected by the fuel consumption and time rationing, is expressed as

$$\sum_{t=1}^{t_{\max}} Le_t \leq Le_{\text{total}}, \quad (5)$$

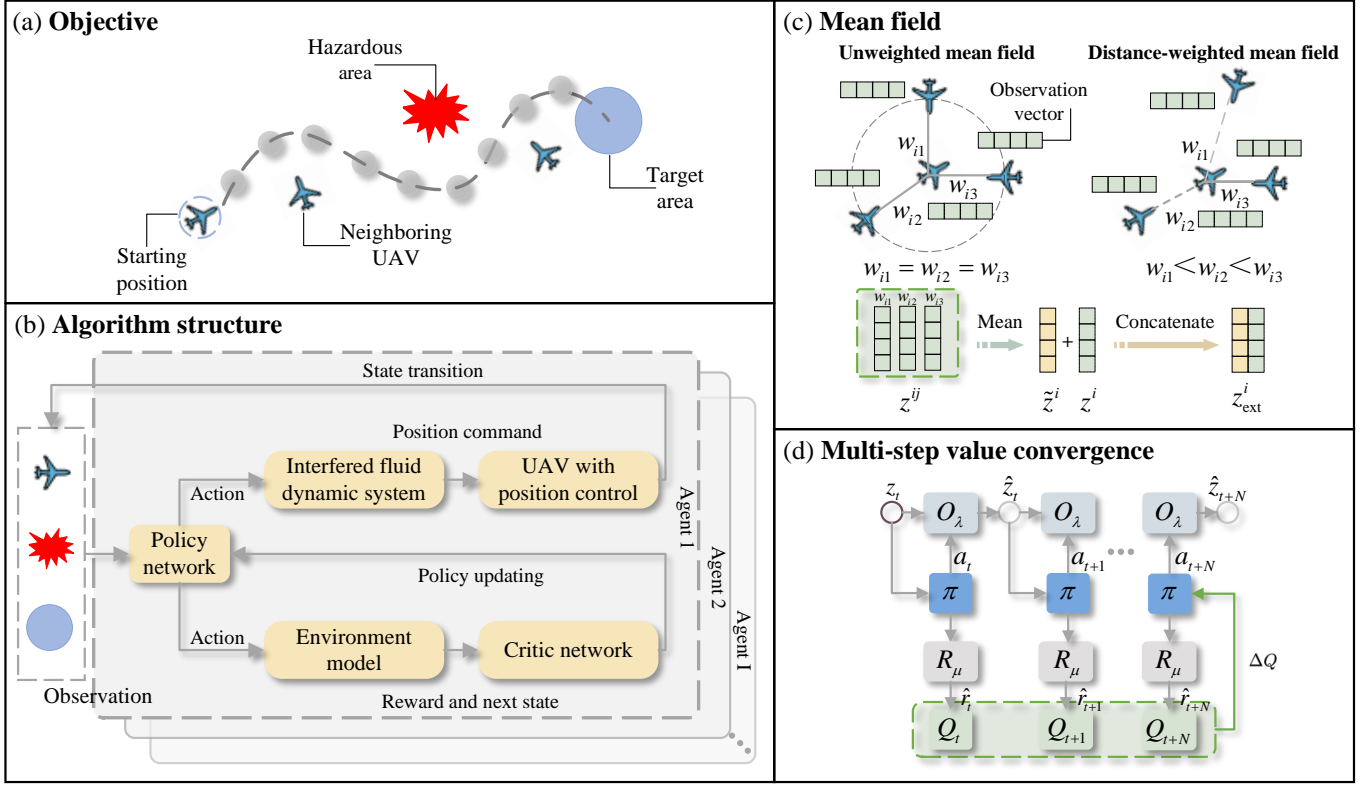


Figure 2. An overview of our study. (a) Illustration of the objective in this paper. Each UAV should achieve its target area while avoiding hazardous areas and collisions with neighboring UAVs. (b) The decision-making and training process of the UAV for path planning. (c) Comparison between unweighted mean field and distance-weighted mean field. (d) Description of the prediction and training process for the multi-step value convergence method in MARL.

where  $t_{\max}$  is the maximum flight time and  $Le_{\text{total}}$  is the maximum total path length. Penalizing constraint violations by the reward function designed in Section IV-A, we allow the UAVs to perform path planning under the constraints above.

#### IV. METHODOLOGY

Many MARL methods are often limited in multi-UAV tasks by the lack of consideration of uncertain changes or the need for extensive agent-environment interactions. Due to the uncertainty in the stochastic environment, it is crucial to design an online obstacle avoidance method for complex tasks. Therefore, we propose CTPDE, which contains a centralized planner without expert experience. Considering the cost and constraints of communication presented in the study, we present CTFDE, which allows UAVs to combine information on their neighbors efficiently through extended observations. The method provides higher training efficiency by introducing a multi-step value convergence approach. The overview is shown in Figure 2, including the objective, algorithm structure, distance-weighted mean field method, and multi-step value convergence approach in our study.

##### A. Centralized Training with Partially Decentralized Execution Decision Process

The state includes information on each UAV, which is described as

$$s^i = (p^i, p^{i,s}, p^{i,e}, v^i), \quad (6)$$

where  $p^{i,s}, p^{i,e}$  denote the starting and ending position of UAV  $i$ , respectively. To enable UAVs to plan feasible and safe paths in the stochastic environment, we propose CTPDE, where UAVs can communicate with the centralized planner and do not require communication among themselves. In this method, the local observation of the UAV contains information on neighboring hazardous areas, which can be set in the following form:

$$z^i = (p^i, p^k, p^{i,s}, p^{i,e}, v^i), \quad (7)$$

where  $p^k, k \in \mathcal{N}^i$  is the position of its neighboring hazardous area  $k$ . The action space can be set in the following form:

$$a^i = (\psi^i, \theta^i, \varphi^i), \quad (8)$$

where  $\psi^i, \theta^i, \varphi^i$  denote the yaw, pitch, and roll of UAV  $i$ , respectively. In the online decision-making process as shown in Fig. 2(b), we calculate the position command of each UAV by the interfered fluid dynamic system (IFDS) algorithm [27]. We adopt  $\psi^i, \theta^i, \varphi^i$  to calculate the repulsive parameter  $\eta_{ic}$ , tangential parameter  $\tau_{ic}$ , and tangent vector  $\kappa$ , where  $c \in [j, k]$  denotes neighboring UAV  $j$  or neighboring hazardous area  $k$ . The parameters can be described as

$$\begin{aligned} \eta_{ic} &= \exp \left[ 1 - \frac{1}{\|p^i - p^{i,e}\| (\|p^i - p^c\| - \rho_{ic})} \right] \psi^i, \\ \tau_{ic} &= \exp \left[ 1 - \frac{1}{\|p^i - p^{i,e}\| (\|p^i - p^c\| - \rho_{ic})} \right] \theta^i, \\ \kappa &= [\cos \varphi^i \sin \varphi^i 0]^T, \end{aligned} \quad (9)$$

where  $\rho_{ij} = 2\rho_u$  and  $\rho_{ik} = \rho_u + \rho_o$ . The next planned position  $\bar{p}^i$  can be obtained as follows:

$$\bar{p}^i = p^i + \left[ \sum_{j \in \mathcal{N}^i} \bar{u}(\eta_{ij}, \tau_{ij}, \kappa) + \sum_{k \in \mathcal{N}^i} \bar{u}(\eta_{ik}, \tau_{ik}, \kappa) \right] \Delta T, \quad (10)$$

where  $\bar{u}(\cdot)$  is the disturbed fluid speed function in [27], and  $\Delta T$  is the sampling time. By entering  $\bar{p}^i$  into the position controller, UAV  $i$  completes path planning for the next moment. For CTPDE, the calculation of  $\bar{p}^i$  is executed by the centralized planner, which connects the positions and desired angles of all UAVs to output the position command for each UAV at the next moment. We design the avoidance reward for leading UAVs to avoid hazardous areas and collisions with neighboring UAVs. The avoidance reward is set in the following form:

$$r_{\text{avo}} = r_{\text{avo},1} + r_{\text{avo},2}. \quad (11)$$

If UAV  $i$  enters the threat zone of its neighboring hazardous area  $k$  ( $\|p^i - p^k\| < \rho_{ik} + d_{\text{thr}}$ ), there is

$$r_{\text{avo},1} = \frac{\|p^i - p^k\| - (\rho_{ik} + d_{\text{thr}})}{\rho_{ik}} - r_a. \quad (12)$$

If UAV  $i$  enters the threat zone of its neighboring UAV  $j$  ( $\|p^i - p^j\| < \rho_{ij} + d_{\text{thr}}$ ), there is

$$r_{\text{avo},2} = \frac{\|p^i - p^j\| - (\rho_{ij} + d_{\text{thr}})}{\rho_{ij}} - r_a, \quad (13)$$

where  $d_{\text{thr}}$  is a threat distance. By setting the threat zone, we keep UAV  $i$  staying as far away from its neighboring hazardous areas and UAVs as possible. In path planning, UAVs need to avoid collisions while achieving shorter pathfinding. The intrinsic reward can be described as

$$r_{\text{int}} = \begin{cases} -\frac{\|p^i - p^{i,e}\|}{\|p^{i,s} - p^{i,e}\|} + r_b & \|p^i - p^{i,e}\| < d_{\text{com}} \\ -\frac{\|p^i - p^{i,e}\|}{\|p^{i,s} - p^{i,e}\|} & \text{otherwise} \end{cases}, \quad (14)$$

where  $d_{\text{com}}$  is a distance threshold for completion, and if for  $\forall i$ ,  $\|p^i - p^{i,e}\| < d_{\text{com}}$ , all UAVs reach their target areas. If UAV  $i$  violates the three-dimensional path constraints described in (3)–(5), then  $r_{\text{con}} = -r_c$ , otherwise  $r_{\text{con}} = 0$ .  $r_a, r_c$  are constant rewards and  $r_b$  is the additional reward for pathfinding completion. The final reward for path planning is a linear operation consisting of the intrinsic reward, avoidance reward, and constraint reward, which can be calculated as

$$r_{\text{path}} = r_{\text{int}} + r_{\text{avo}} + r_{\text{con}}. \quad (15)$$

### B. Extended Observation for Fully Decentralized Execution

Considering that UAVs are out of contact with the centralized planner and can communicate with their neighboring UAVs, we propose CTFDE, which quantifies the varying strengths of interactions among UAVs. In this method, the observation of the UAV  $i$  contains information on its neighboring hazardous areas and UAVs. Inspired by the mean field approach [28], we design the distance-weighted mean field

method to establish the extended observation, which can be denoted as

$$z_{\text{ext}}^i = (z^i, \tilde{z}^i), \tilde{z}^i = \frac{1}{W_i} \sum_{j \in \mathcal{N}^i} w_{ij} z^j, \\ W_i = \sum_{j \in \mathcal{N}^i} w_{ij}, w_{ij} \propto \frac{1}{\|p^i - p^j\|}, \quad (16)$$

where  $w_{ij}$  denotes the weight between UAV  $i$  and UAV  $j$ , responding to the distance between them. If the distance is smaller, we consider the strength of interaction between UAV  $i$  and UAV  $j$  to be stronger, which means they should pay more attention to the collision with each other. In addition, the action  $a^i$ , reward  $r^i$ , and next planned position  $\bar{p}^i$  of UAV  $i$  can be calculated similarly to CTPDE proposed in Section IV-A. However, in CTFDE, it is worth noting that the next planned position  $\bar{p}^i$  can be calculated by each UAV itself. Therefore, this method allows the UAV to make a fully decentralized execution without relying on the centralized planner. The decentralized policy function of MADDPG can be approximated in the following form:

$$\pi^i(z_{\text{ext}}^i) \sim \tilde{\pi}^i(z^i, \tilde{z}^i). \quad (17)$$

Next, we will mathematically prove why this approximation holds.

*Theorem 1 (Distance-weighted mean field approximation):* When considering agent  $i$ , the decentralized policy function  $\pi^i(z_{\text{ext}}^i)$  can be approximated by  $\tilde{\pi}^i(z^i, \tilde{z}^i)$ .

*Proof 1:* Since

$$\tilde{z}^i = \frac{1}{W_i} \sum_{j \in \mathcal{N}^i} w_{ij} z^j, W_i = \sum_{j \in \mathcal{N}^i} w_{ij}, \quad (18)$$

we regard each  $z^j, j \in \mathcal{N}^i$  as the sum of  $\tilde{z}^i$  and a small fluctuation  $\delta z_{ij}$ , which can be denoted as

$$z^j = \tilde{z}^i + \delta z_{ij}, \quad (19)$$

therefore, we have:

$$\frac{1}{W_i} \sum_{j \in \mathcal{N}^i} w_{ij} \delta z_{ij} = \frac{1}{W_i} \sum_{j \in \mathcal{N}^i} w_{ij} (z^j - \tilde{z}^i) = \tilde{z}^i - \tilde{z}^i = 0. \quad (20)$$

We expand the decentralized policy function according to [29], considering the interactions among its neighboring UAVs, which can be described as

$$\pi^i(z_{\text{ext}}^i) = \frac{1}{W_i} \sum_{j \in \mathcal{N}^i} w_{ij} \tilde{\pi}^i(z^i, z^j) \\ = \frac{1}{W_i} \sum_{j \in \mathcal{N}^i} w_{ij} \tilde{\pi}^i(z^i, \tilde{z}^i + \delta z_{ij}). \quad (21)$$

We denote  $\tilde{\pi}^i(z^i, \tilde{z}^i)$  as  $\pi_0$ . It expands each term in the sum according to Taylor's formula, which can be calculated in the following form:

$$\begin{aligned}
(21) &= \frac{1}{W_i} \sum_{j \in \mathcal{N}^i} w_{ij} \left( \pi_0 + \nabla_{\tilde{z}^i} \pi_0 \delta z_{ij} + \frac{1}{2} \delta z_{ij} \nabla_{\tilde{z}^i}^2 \pi_0 \delta z_{ij} \right) \\
&= \pi_0 + \frac{1}{W_i} \sum_{j \in \mathcal{N}^i} w_{ij} \nabla_{\tilde{z}^i} \pi_0 \delta z_{ij} \\
&\quad + \frac{1}{2W_i} \sum_{j \in \mathcal{N}^i} w_{ij} \delta z_{ij} \nabla_{\tilde{z}^i}^2 \pi_0 \delta z_{ij} \\
&= \pi_0 + 0 + \frac{1}{2W_i} \sum_{j \in \mathcal{N}^i} w_{ij} \delta z_{ij} \nabla_{\tilde{z}^i}^2 \pi_0 \delta z_{ij} \\
&\approx \pi_0 = \tilde{\pi}^i(z^i, \tilde{z}^i). \tag{22}
\end{aligned}$$

Hence, based on (18)–(22), the decentralized policy function  $\pi^i(z_{\text{ext}}^i)$  can be approximated by  $\tilde{\pi}^i(z^i, \tilde{z}^i)$  with second order small error.

### C. Model Predictive Control–Based Multi-Agent Reinforcement Learning

The reference [30] proposes the formula of basic MPC and basic MPC with added terminal cost. By combining RL and MPC, we can obtain the following forms by transforming the problem from least cost to most benefit:

$$\pi_1(z_t) = \arg \max_{a_{t:t+N}} \mathbb{E} \left[ \sum_{c=t}^{t+N-1} \gamma^c R(z_c, a_c) \right], \tag{23}$$

$$\begin{aligned}
\pi_2(z_t) &= \arg \max_{a_{t:t+N}} \mathbb{E} \left[ \sum_{k=t}^{t+N-1} \gamma^k R(z_c, a_c) \right. \\
&\quad \left. + \gamma^{t+N} \max Q_{\omega^-}(z_{t+N}, a_{t+N}) \right], \tag{24}
\end{aligned}$$

where  $\arg \max_x G(x)$  represents the value of variable  $x$  when  $G(x)$  obtains its maximum value. According to (23), the approach executes one step convergence with the short-term reward  $R(z_c, a_c)$ . In prior work [25], we improved the single-agent RL method based on MPC, illustrated the difference between the method and  $n$ -step temporal difference, and theoretically proved an optimal fixed step  $N$ . Considering a multi-UAV pathfinding scenario, we further extend the above work to a multi-agent RL method. Additionally, we propose a dynamic adaptive step  $N$  to reduce the cumulative errors arising from the virtual environment model.

To enhance the learning efficiency and sample utilization of agents in MARL, we adopt an improved MARL method based on MPC. This method applies a rolling optimization approach to maximize the cumulative return in each prediction interval. Since the value function  $Q_{\omega}(z_c, a_c)$  can be approximated by the cumulative rewards  $\sum_{m=c}^{\infty} \gamma^m r_m$ , we conduct multi-step value convergence by replacing the reward  $R(z_c, a_c)$  with the rewards  $\sum_{m=k}^{\infty} \gamma^m r_m$  in (23) to maximize both short-term and long-term rewards. The strategy of each agent can be described in the following form:

$$\pi_3(z_t) = \arg \max_{a_{t:t+N}} \mathbb{E} \left[ \sum_{c=t}^{t+N} \gamma^c \left( \sum_{m=c}^{\infty} \gamma^m r_m \right) \right]. \tag{25}$$

In (25), we perform predictive control based on a single moment  $t$  to produce a local optimal solution. The rolling optimization is then performed in the next  $N$  steps to generate multiple local optimal solutions and calculate the optimal value. The use of cumulative rewards compensates for the lack of the terminal reward. Although the multi-step value convergence approach increases the computational complexity during training, it can improve the sample utilization and training efficiency by accumulating the cumulative rewards in the next  $N$  steps. The loss function in (1) is improved as follows:

$$L_{\omega}^i = \mathbb{E}_{(z_c, a_c) \sim \mathcal{B}} \sum_{n=0}^{N-1} \|Q_{\omega}^i(z_{c+n}, a_{c+n}) - y_{c+n}^i\|^2. \tag{26}$$

According to (24), the  $Q$ -target is modified as follows:

$$\begin{aligned}
y_{c+n}^i &= \sum_{m=n}^{N-1} \gamma^{m-n} \hat{r}_{c+m} \\
&\quad + \gamma^{N-n} \max Q_{\omega^-}^i(z_{c+N}, a_{c+N}). \tag{27}
\end{aligned}$$

In addition, the method builds a virtual environment model for assisting rolling predictions during policy learning, which includes an observation transition network  $O_{\lambda}$  and a reward network  $R_{\mu}$ . We use  $\hat{z}, \hat{r}$  to denote the joint observations and reward generated from the virtual model, respectively. The loss functions are shown below:

$$\begin{aligned}
L_{\lambda} &= \mathbb{E}_{(z_c, a_c) \sim \mathcal{B}} \|(\hat{z}_{c+1} - z_{c+1})\|^2, \\
L_{\mu} &= \mathbb{E}_{(z_c, a_c) \sim \mathcal{B}} \|(\hat{r}_c - r_c)\|^2. \tag{28}
\end{aligned}$$

They indicate the degree of deviation between the constructed virtual model and the environment. By minimizing the values of these functions, the virtual model can increasingly approximate the environment. The value of the prediction step  $N$  affects the performance of our method. When the model's approximation to the environment is inaccurate, a larger  $N$  can lead to cumulative errors in multi-step convergence. Therefore, we describe the degree of deviation  $F(z_c, a_c)$  between the model and environment through the loss functions in (28), which is calculated as

$$F(z_c, a_c) = \epsilon_1 L_{\lambda} + (1 - \epsilon_1) L_{\mu}, \tag{29}$$

where  $\epsilon_1$  is the weighting factor between the observation transition network  $O_{\lambda}$  and reward network  $R_{\mu}$ . Furthermore, instead of the conventional fixed-step method, the prospective value of  $N$  can be improved as follows:

$$N(z_c, a_c) = \lfloor -\epsilon_2 F(z_c, a_c) + N_{\text{base}} \rfloor, \tag{30}$$

where  $\epsilon_2$  is a weighting factor and  $N(z_c, a_c)$  is an integer limited in  $[1, N_{\text{max}}]$ . Subscripts base and max are the settled based and maximum values, respectively.  $\lfloor x \rfloor = \max \{m \in \mathbb{Z} | m \leq x\}$ , where  $x \in \mathbb{R}$  and  $\mathbb{Z}$  denotes the set of integers. Based on the above adaptive approach, we can reduce the cumulative errors by shortening the prediction step  $N$  when the model is poorly fitted. In addition, we set a maximum value  $N_{\text{max}}$  to prevent the computational complexity caused by over-prediction.

The flowchart of the MPC-based MARL approach is shown in Algorithm 1. We use the samples selected from the experience replay buffer to update the virtual environment model

---

**Algorithm 1** MPC-Based MARL
 

---

**Input:** Discount factor( $\gamma$ ); Learning rate( $\alpha$ );  
 Training episode( $E$ ); Training step( $T$ );  
 Stochastic noise( $\mathfrak{N}$ ); Prediction step( $N$ );

**Output:** Policy network( $\pi_\beta^i$ )

```

1: Initialize networks  $\omega, \beta, \lambda, \mu$  and the replay buffer  $\mathcal{B}$ ;
2: for all  $e = 1 \rightarrow E$  do
3:   Get the initial observation  $z_0$ ;
4:   for all  $t = 0 \rightarrow T$  do
5:      $a_t^i \leftarrow \pi_\beta^i(z_t^i), \mathfrak{N}$ , for all  $i$ ;  $\triangleright$  on-policy action
6:      $r_t, z_{t+1} \leftarrow Env$ ;  $\triangleright$  transition in environment
7:      $\mathcal{B} \leftarrow (z_t, a_t, r_t, z_{t+1})$ ;  $\triangleright$  replay buffer update
8:     Randomly select  $\|\mathcal{B}\|$  samples  $(z_c, a_c, r_c, z_{c+1})$  from  $\mathcal{B}$ ;
9:     for all  $i = 1 \rightarrow I$  do
10:       $\hat{z}_{c+1}, \hat{r}_c \leftarrow$   $\triangleright$  prediction in model
11:       $O_\lambda(z_c, a_c), R_\mu(z_c, a_c)$ ;
12:       $N(z_c, a_c) \leftarrow \text{Eq. (30)}$ 
13:      for all  $n = 1 \rightarrow N(z_c, a_c)$  do
14:         $a_{c+n}^i \leftarrow \pi_\beta^i(\hat{z}_{c+n}^i)$ , for all  $i$ ;
15:         $\hat{z}_{c+n+1}, \hat{r}_{c+n} \leftarrow$   $\triangleright$  multi-step prediction
16:         $O_\lambda(\hat{z}_{c+n}, a_{c+n}), R_\mu(\hat{z}_{c+n}, a_{c+n})$ ;
17:      end for
18:       $L_\omega^i \leftarrow \text{Eq. (26)}$ ;
19:       $L_\beta^i \leftarrow \text{Eq. (2)}$ ;
20:      Refresh networks  $\omega^i, \beta^i$ ;  $\triangleright$  gradient-descent
21:    end for
22:     $L_\lambda, L_\mu \leftarrow \text{Eq. (28)}$ ;
23:    Refresh networks  $\lambda, \mu$ ;  $\triangleright$  gradient-descent
24:  end for
  
```

---

and each UAV's policy. Meanwhile, the virtual model has a facilitating effect on the update of each UAV's policy in Fig. 2(d). Next, we will conduct validation experiments in simulations and real-robot systems.

## V. EXPERIMENTS

In this section, extensive experiments are conducted to evaluate the performance of CTPDE and CTFDE for solving the obstacle avoidance problem in the stochastic environment. We build a multi-UAV simulation platform capable of real-world gravity, drag, and other irresistible factors, as shown in Fig. 3. In comparison experiments, we adopt various baselines including RRT\* [5], ACO [6], and decentralized DDPG [25]. We verify the influence of the extended observation and MPC-based MARL approach in the ablation studies considering the communication constraint with the centralized planner. Moreover, we apply the policy network trained under a small size to solve larger ones to investigate the generalization of our method. Finally, we conduct offline training with our method based on the simulation platform and execute online decision-making in the real-robot system.

### A. Setting Up

Before analyzing the comparative results, we first introduce the detailed settings in simulations. We assume an instance

has six UAVs that will arrive at four destinations according to specific policies. The corresponding destination of each UAV can be seen in Fig. 3(a). The environment can detect a specific number (3 to 5) of locations of hazardous areas at regular intervals, as seen in Fig. 3(b). Each UAV can only communicate with the centralized planner or its neighboring UAVs. UAVs should plan safe paths to avoid collisions, avoid entering hazardous areas, and finally reach their destinations. We conduct these simulations on a server with a Windows 10 operating system, Intel Core i7-11700 CPU, 16-GB memory, and Radeon 520 GPU. All simulation programs are developed based on Python 3.7 and PyCharm 2022.2.3 compiler. In our methods, the discount factor  $\gamma$  and update factor  $\zeta$  are 0.99, the learning rate  $\alpha$  is 0.001, and the batch size  $\|\mathcal{B}\|$  is 128. We train the policy in simulations for  $E = 30$  episodes in 100 randomly generated instances. The changing interval of hazardous areas is fixed at 15 in the training process. To plot experimental curves, we adopt solid curves to depict the mean of all instances and shaded regions corresponding to standard deviation among instances.

### B. Comparison Analysis

In the training process, we employ CTPDE and CTFDE to improve the performance of pathfinding strategies. We compare the training methods with the decentralized DDPG (Dec-DDPG) method. In addition, we further deploy the policy networks trained by our methods in 100 different instances and compare them with non-learning approaches including RRT\* and ACO. The baselines are briefly introduced as follows.

- 1) RRT\*: The algorithm uses the bias sampling method based on the artificial potential field function proposed in [5], and extends the tree to obtain the heuristic path.
- 2) ACO: The algorithm introduces a chaotic-polarized-simulated scheme [6], and performs state transfer through pheromone concentration to achieve pathfinding.
- 3) Dec-DDPG: The method considers each UAV as an independent agent and uses DDPG [25] to train a separate obstacle avoidance strategy.

The learning curves of our methods and Dec-DDPG are presented in Fig. 4, where the horizontal axis refers to the number of episodes, and the vertical axis refers to the episode returns calculated by (15). We can observe that the policies in Dec-DDPG converge to a poorer value due to the lack of a centralized critic. Among these learning-based approaches, CTPDE shows the fastest convergence to the local optimal value. In this method, the centralized planner connects the observations of all UAVs and makes decisions with more information. Compared to CTPDE, CTFDE leads UAVs' policies to converge to sub-optimal values.

We propose two additional evaluation metrics: computation time and collision times. Computation time refers to the total time required for path planning for all UAVs. Collision times refer to the number of times all UAVs enter hazardous areas or collide with their neighboring UAVs. The average experiment results of 100 instances are shown in Table I. The table gathers the computation time (Ti.), episode returns (Re.), and collision times (Co.) of all methods. It analyzes the influence of three



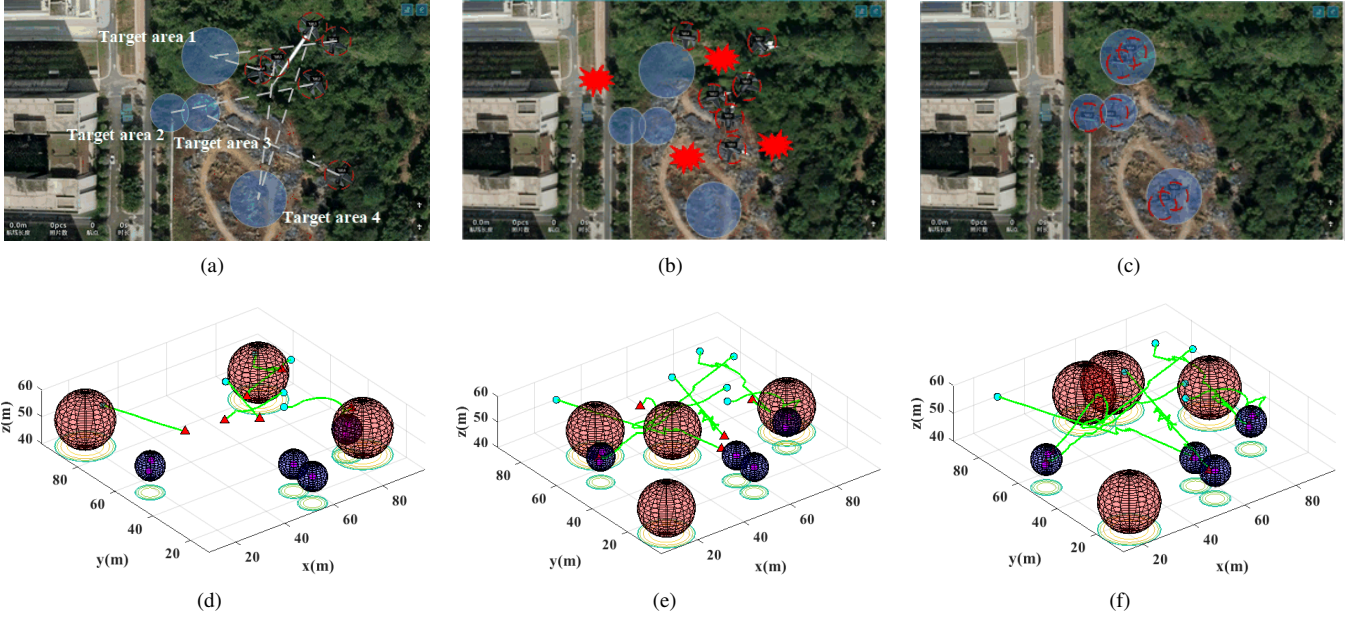


Figure 3. Six-UAV path planning in the simulation platform. (a)–(c) show the whole process of path planning in the simulation. (d)–(f) are the real-time trajectories for UAV path planning.

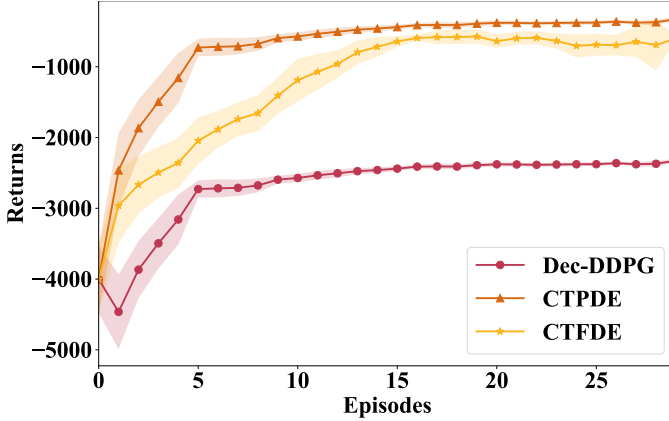


Figure 4. Learning curves of our method and Dec-DDPG.

changing intervals (5, 10, and 15) of hazardous areas, which are termed as V5, V10, and V15, respectively. We can observe that there is a relationship between the collision times and episode returns, which are calculated by the reward function in this study. UAVs train their strategies to achieve higher returns, which leads to fewer collision times in the pathfinding. Although ACO provides the best solution, it takes the most computation time due to the algorithm's iterations with the changes in hazardous areas. In addition, the computation time increases significantly as the changing interval is reduced. Compared to ACO, RRT\* saves computation time through fast search, its scalability gradually deteriorates as the changing interval increases. The episode returns of CTPDE and CTFDE are slightly lower than those of ACO, which means the longer paths are calculated using these two methods. However, the methods save a large amount of computational resources and maintain favorable performance at different intervals. As a

Table I  
EXPERIMENT RESULTS OF BASELINES AND OUR METHODS.

Interval	Method	Ti.(s)	Re.	Co.
V15	RRT*	1.97	-803	0
	ACO	3.88	-795	0
	Dec-DDPG	0.94	-2689	10
	CTPDE	1.03	-825	0
	CTFDE	1.05	-924	0
V10	RRT*	2.52	-1027	1
	ACO	5.61	-811	0
	Dec-DDPG	1.04	-2732	11
	CTPDE	1.25	-846	0
	CTFDE	1.30	-985	0
V5	RRT*	3.99	-1262	2
	ACO	9.86	-857	0
	Dec-DDPG	1.27	-2793	13
	CTPDE	1.59	-876	0
	CTFDE	1.68	-1001	0

result, our methods plan feasible and safe paths for UAVs in a shorter solved time.

### C. Ablation Study

In CTFDE, we design the extended observation enabling each UAV to combine information on its neighboring agents based on the distance-weighted mean field approach. In addition, we adopt an improved MARL method conducting multi-step value convergence to reduce agent-environment interactions. We perform ablation studies to verify the influence of the extended observation and MPC-based MARL approach considering the communication constraint with the centralized planner. The learning curves are shown in Fig. 5, where "CTFDE-MPC" refers to adopting the MPC-based MARL



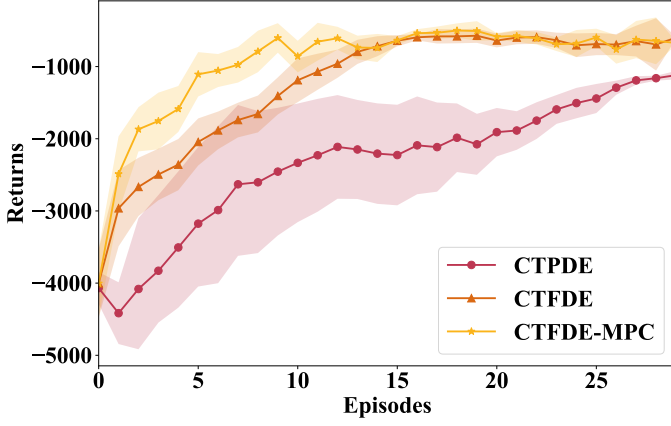


Figure 5. Ablation study results of our methods.

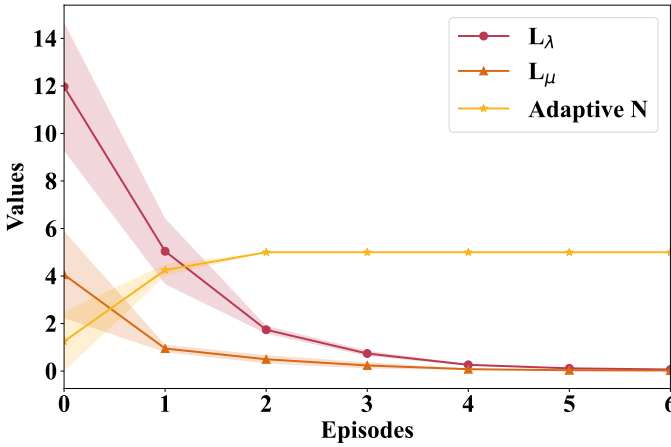


Figure 6. The curves of  $L_\lambda$ ,  $L_\mu$ , and  $N$  for CTFDE-MPC.  $\epsilon_1$  in (29) is 0.25.  $\epsilon_2$ ,  $N_{\text{base}}$ , and  $N_{\text{max}}$  in (30) are 0.66, 6, and 5, respectively.

method in CTFDE. We can observe that although CTPDE is more efficient in Fig. 4, it is limited when the communication between UAVs and the centralized planner is interrupted. The convergence speed for CTPDE decreases significantly and eventually converges to a sub-optimal value. In contrast, the results verify that CTFDE maintains favorable performance under communication constraints. In addition, it highlights that CTFDE-MPC can significantly reduce the episodes required for the strategies to converge to the local optimal values. Moreover, we plot the average value of the prediction step  $N$  for CTFDE-MPC in Fig. 6. The horizontal coordinate refers to the number of episodes, and the vertical coordinate refers to the values of the loss function  $L_\lambda$ , loss function  $L_\mu$ , and prediction step  $N$ , which are calculated on average in each episode. Through constant training, the values of  $L_\lambda$  and  $L_\mu$  gradually decrease to 0, which means the model has an increasing approximation to the environment. Therefore, a more accurate model brings the prediction step  $N$  higher, prompting the enhancement of learning efficiency in CTFDE. The results demonstrate that MPC-based MARL approach can effectively speed up the learning process and reduce the expansive agent-environment interactions in convergence.

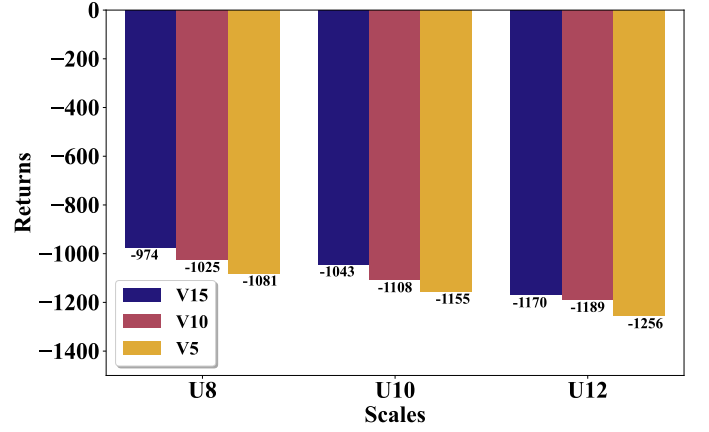


Figure 7. Generalization to larger-scale instances.

#### D. Generalization to Larger-Size Instances

In larger-size multi-agent pathfinding scenarios, we will lose extensive computational resources by retraining the planning strategies. Therefore, we expect that our trained model holds favorable generalization performance. This study proposes the CTFDE method, where the decentralized policies of agents can be deployed directly to other agents without retraining. Here, we employ the trained pathfinding networks to solve the instances with more agents to verify the generalization performance of our method. Three scenarios including eight UAVs (termed as U8), ten UAVs (termed as U10), and twelve UAVs (termed as U12) are considered in our experiments. The generalization results are shown in Fig. 7, where the horizontal axis refers to the scenario sizes, and the vertical axis refers to the episode returns. The legend refers to the changing intervals of hazardous areas. We can observe that due to the increase in scale, UAVs have a rising difficulty in path planning and achieve lower returns. However, it can maintain favorable solution quality and computation efficiency against the baselines.

The average experiment results are shown in Table II, which displays the computation time (Ti.), episode returns (Re.), and collision times (Co.) testing in different instance scales. As can be seen, CTFDE outperforms RRT\*, ACO, and Dec-DDPG in all instances. RRT\* and ACO still suffer from low scalability and high time consumption, respectively, especially in larger-size scenes. In addition, in large-scale dynamic scenarios such as U12 & V5, the CTFDE-trained policies still maintain excellent performance, with similar returns to ACO at low computational loss. It is worth noting that since CTFDE employs a decentralized decision-making approach, its solution time does not change significantly with increasing size. The results demonstrate that the trained policies under small-scale instances can perform feasible and safe path planning in various-scale scenarios. Therefore, our method has a strong generalization on the path planning problem in the stochastic environment.

#### E. Deployment in Real-Robot System

To verify the adaptability of CTFDE in the real world, we conduct experiments with actual UAVs. In the simulation

Table II  
GENERALIZATION RESULTS OF BASELINES AND OUR METHOD.

Interval	Method	U8			U10			U12		
		Ti.(s)	Re.	Co.	Ti.(s)	Re.	Co.	Ti.(s)	Re.	Co.
V15	RRT*	2.46	-861	0	4.02	-951	0	7.13	-1178	1
	ACO	5.57	-817	0	9.39	-870	0	18.16	-1004	0
	Dec-DDPG	0.95	-2759	10	0.98	-2872	11	0.99	-3080	13
	CTFDE	1.06	-974	0	1.06	-1043	0	1.08	-1130	0
V10	RRT*	4.05	-1123	1	6.82	-1295	2	11.01	-1502	3
	ACO	8.37	-854	0	14.76	-903	0	27.84	-1066	0
	Dec-DDPG	1.07	-2808	11	1.07	-2961	12	1.10	-3174	15
	CTFDE	1.32	-1025	0	1.34	-1108	0	1.35	-1189	0
V5	RRT*	5.77	-1364	3	8.95	-1582	4	14.58	-1867	6
	ACO	13.72	-912	0	23.09	-977	0	39.16	-1131	0
	Dec-DDPG	1.26	-2869	11	1.27	-3044	13	1.29	-3263	16
	CTFDE	1.66	-1081	0	1.69	-1155	0	1.70	-1256	0

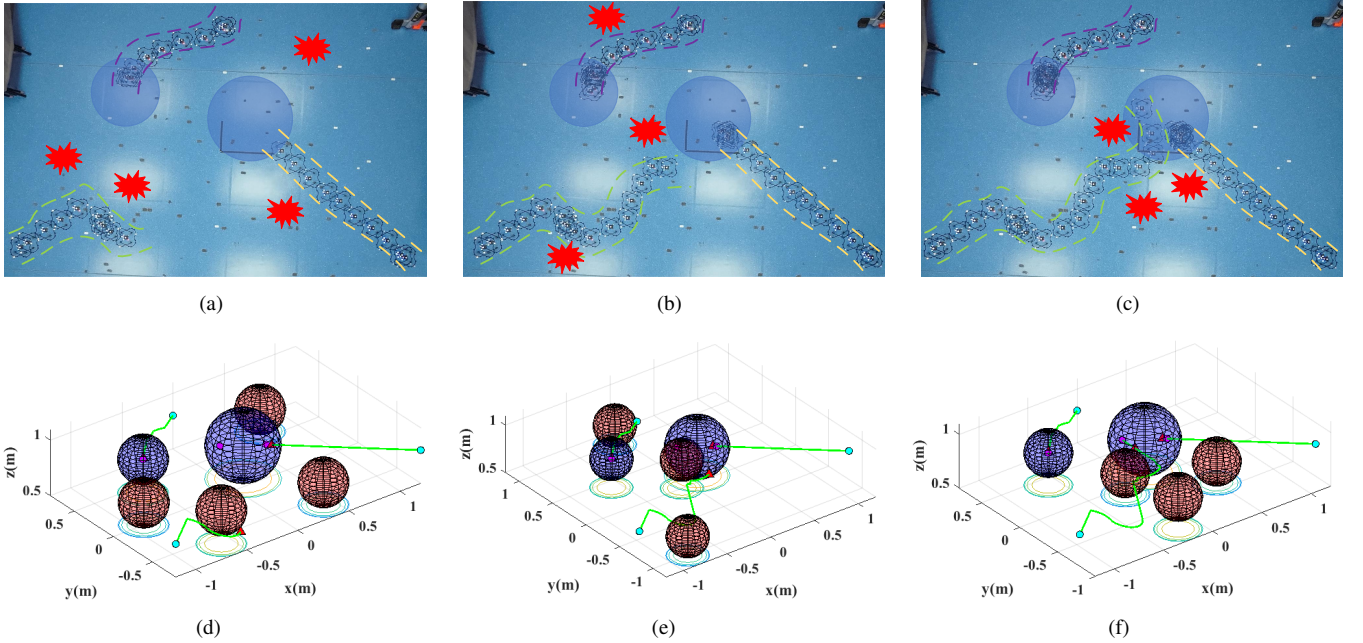


Figure 8. Three-UAV path planning in the real-robot platform. (a)–(c) show the whole process of path planning in the real-robot system. (d)–(f) are the real-time trajectories for UAV path planning. We execute online decision-making in experiments based on the policies training with CTFDE in simulations.

environment, we simulate obstacle avoidance scenarios in the actual mission, including the UAV dynamics model and the stochastic environment. In experiments shown in Fig. 8, we consider three UAVs' pathfinding for obstacle avoidance in the stochastic environment. By performing CTFDE-MPC training in simulations, we can get the policy networks of UAVs in this scenario. Our algorithm receives messages from Optitrack, including the positions of all UAVs and hazardous areas. Then the algorithm calculates the observation of each UAV and outputs the position command with policy networks, which is sent to the ground control system. Based on these networks, UAVs can avoid hazardous areas and reach the target areas in experiments while ensuring they do not collide. The experiments' success verifies that the designed method can accomplish multi-UAV obstacle avoidance by offline training and online decision-making, and this MARL method

is improved based on MPC.

## VI. CONCLUSIONS

This paper has presented a novel centralized training with decentralized execution method for multi-UAV obstacle avoidance. It has designed a CTFDE approach to plan feasible paths for UAVs in the stochastic environment. By evolving from partially to fully decentralized execution, we have proposed a CTFDE approach to overcome the communication constraint. The approach has established an extended observation for each UAV based on the distance-weighted mean field method, enabling each UAV to combine information on its neighbors efficiently. With this approach, UAVs have completed obstacle avoidance tasks without relying on the centralized planner and only through their extended observations. Moreover, we have proposed the CTFDE-MPC method to improve the

agent's learning efficiency and reduce the expensive agent-environment interactions in convergence. The experiment results have shown that our method achieves favorable solution quality and computation efficiency against the baselines, especially in high-dynamic instances. We have demonstrated the influence of the extended observation and MPC-based MARL approach via ablation studies. Furthermore, the generalization and adaptability of our method have been verified by applying a trained model to larger-size instances and real-robot systems, respectively.

## REFERENCES

- [1] J. Lü, F. Chen, and G. Chen, "Nonsmooth leader-following formation control of nonidentical multi-agent systems with directed communication topologies," *Automatica*, vol. 64, pp. 112–120, 2016.
- [2] L. Ji, X. Yu, and C. Li, "Group consensus for heterogeneous multiagent systems in the competition networks with input time delays," *IEEE Trans. Syst. Man Cybern.: Syst.*, vol. 50, no. 11, pp. 4655–4663, 2018.
- [3] K. Ze, W. Wang, K. Liu, and J. Lü, "Time-varying formation planning and distributed control for multiple uavs in clutter environment," *IEEE Trans. Ind. Electron.*, vol. 71, no. 9, pp. 11 305–11 315, 2023.
- [4] L. Heuer, L. Palmieri, A. Rudenko, A. Mannucci, M. Magnusson, and K. O. Arras, "Proactive model predictive control with multi-modal human motion prediction in cluttered dynamic environments," in *Proc. Int. Conf. Intell. Robots Syst. (IROS)*. IEEE, 2023, pp. 229–236.
- [5] Y. Guo, X. Liu, Q. Jia, X. Liu, and W. Zhang, "Hpo-rrt\*: A sampling-based algorithm for uav real-time path planning in a dynamic environment," *Complex & Intell. Syst.*, vol. 9, no. 6, pp. 7133–7153, 2023.
- [6] M. Yan, C. A. Chan, A. F. Gygax, C. Li, A. Nirmalathas, and I. Chih-Lin, "Efficient generation of optimal uav trajectories with uncertain obstacle avoidance in mec networks," *IEEE Internet Things J.*, early access, Aug., 2024.
- [7] Z. Liu, Y. Zhang, C. Yuan, L. Ciarletta, and D. Theilliol, "Collision avoidance and path following control of unmanned aerial vehicle in hazardous environment," *J. Intell. Robot. Syst.*, vol. 95, pp. 193–210, 2019.
- [8] E. Kaufmann, L. Bauersfeld, A. Loquercio, M. Müller, V. Koltun, and D. Scaramuzza, "Champion-level drone racing using deep reinforcement learning," *Nature*, vol. 620, no. 7976, pp. 982–987, 2023.
- [9] T. Haarnoja, B. Moran, G. Lever, S. H. Huang, D. Tirumala, J. Humplik, M. Wulfmeier, S. Tunyasuvunakool, N. Y. Siegel, R. Hafner *et al.*, "Learning agile soccer skills for a bipedal robot with deep reinforcement learning," *Sci. Rob.*, vol. 9, no. 89, p. eadi8022, 2024.
- [10] L. Zhang, W. Yi, H. Lin, J. Peng, and P. Gao, "An efficient reinforcement learning-based cooperative navigation algorithm for multiple uavs in complex environments," *IEEE Trans. Ind. Inf.*, vol. 20, no. 10, pp. 12 396–12 406, 2024.
- [11] L. Chen, Y. Wang, Z. Miao, Y. Mo, M. Feng, Z. Zhou, and H. Wang, "Transformer-based imitative reinforcement learning for multirobot path planning," *IEEE Trans. Ind. Inf.*, vol. 19, no. 10, pp. 10 233–10 243, 2023.
- [12] M. Damani, Z. Luo, E. Wenzel, and G. Sartoretti, "Primal \_2: Pathfinding via reinforcement and imitation multi-agent learning-lifelong," *IEEE Rob. Autom. Lett.*, vol. 6, no. 2, pp. 2666–2673, 2021.
- [13] Y. Yan, X. Li, X. Qiu, J. Qiu, J. Wang, Y. Wang, and Y. Shen, "Relative distributed formation and obstacle avoidance with multi-agent reinforcement learning," in *Proc. Int. Conf. Robot. Autom. (ICRA)*. IEEE, 2022, pp. 1661–1667.
- [14] J. Bloom, P. Paliwal, A. Mukherjee, and C. Pinciroli, "Decentralized multi-agent reinforcement learning with global state prediction," in *Proc. Int. Conf. Intell. Robots Syst. (IROS)*. IEEE, 2023, pp. 8854–8861.
- [15] H. Guan, Y. Gao, M. Zhao, Y. Yang, F. Deng, and T. L. Lam, "Ab-mapper: Attention and bicnet based multi-agent path planning for dynamic environment," in *Proc. Int. Conf. Intell. Robots Syst. (IROS)*. IEEE, 2022, pp. 13 799–13 806.
- [16] Y. Yang, R. Luo, M. Li, M. Zhou, W. Zhang, and J. Wang, "Mean field multi-agent reinforcement learning," in *Proc. Int. Conf. Mach. Learn. (ICML)*. PMLR, 2018, pp. 5571–5580.
- [17] X. Wang, Z. Ning, L. Guo, S. Guo, X. Gao, and G. Wang, "Mean-field learning for edge computing in mobile blockchain networks," *IEEE Trans. Mob. Comput.*, vol. 22, no. 10, pp. 5978–5994, 2022.
- [18] B. Wang, S. Li, X. Gao, and T. Xie, "Weighted mean field reinforcement learning for large-scale uav swarm confrontation," *Appl. Intell.*, vol. 53, no. 5, pp. 5274–5289, 2023.
- [19] W. Wang, Y. Liu, R. Srikant, and L. Ying, "3m-rl: Multi-resolution, multi-agent, mean-field reinforcement learning for autonomous uav routing," *IEEE Trans. Intell. Transp. Syst.*, vol. 23, no. 7, pp. 8985–8996, 2021.
- [20] R. S. Sutton, "Dyna, an integrated architecture for learning, planning, and reacting," *ACM Sigart Bull.*, vol. 2, no. 4, pp. 160–163, 1991.
- [21] K. Chua, R. Calandra, R. McAllister, and S. Levine, "Deep reinforcement learning in a handful of trials using probabilistic dynamics models," in *Proc. Adv. Neural Inf. Process. Syst.*, vol. 31, 2018, pp. 4754–4765.
- [22] M. Janner, J. Fu, M. Zhang, and S. Levine, "When to trust your model: Model-based policy optimization," in *Proc. Adv. Neural Inf. Process. Syst.*, vol. 16, 2019, pp. 12 487–12 498.
- [23] J. Buckman, D. Hafner, G. Tucker, E. Brevdo, and H. Lee, "Sample-efficient reinforcement learning with stochastic ensemble value expansion," in *Proc. Adv. Neural Inf. Process. Syst.*, vol. 31, 2018, pp. 8224–8234.
- [24] A. Byravan, J. T. Springenberg, A. Abdolmaleki, R. Hafner, M. Neunert, T. Lampe, N. Siegel, N. Heess, and M. Riedmiller, "Imagined value gradients: Model-based policy optimization with transferable latent dynamics models," in *Proc. Mach. Learn. Res.* PMLR, 2020, pp. 566–589.
- [25] Q. Wu, K. Liu, and L. Chen, "Model predictive control-based value estimation for efficient reinforcement learning," *IEEE Intell. Syst.*, vol. 39, no. 3, pp. 63–72, 2024.
- [26] S. Omidshafiei, A.-A. Agha-Mohammadi, C. Amato, and J. P. How, "Decentralized control of partially observable markov decision processes using belief space macro-actions," in *Proc. Int. Conf. Robot. Autom. (ICRA)*. IEEE, 2015, pp. 5962–5969.
- [27] J. Wu, H. Wang, N. Li, and Z. Su, "Formation obstacle avoidance: A fluid-based solution," *IEEE Syst. J.*, vol. 14, no. 1, pp. 1479–1490, 2019.
- [28] D. Chen, Q. Qi, Z. Zhuang, J. Wang, J. Liao, and Z. Han, "Mean field deep reinforcement learning for fair and efficient uav control," *IEEE Internet Things J.*, vol. 8, no. 2, pp. 813–828, 2020.
- [29] Q. Hao, W. Huang, T. Feng, J. Yuan, and Y. Li, "Gat-mf: Graph attention mean field for very large scale multi-agent reinforcement learning," in *Proceedings of the 29th ACM SIGKDD Conference on Knowledge Discovery and Data Mining*, 2023, pp. 685–697.
- [30] C. E. Garcia, D. M. Prett, and M. Morari, "Model predictive control: Theory and practice—a survey," *Automatica*, vol. 25, no. 3, pp. 335–348, 1989.



**Qizhen Wu** received the B.S. degree in aeronautical and astronautical engineering from Sun Yat-sen University, Guangzhou, China, in 2022. He is currently pursuing the Ph.D. degree with the School of Automation Science and Electrical Engineering, Beihang University, Beijing, China. His current research interests include reinforcement learning, robotic control, and swarm confrontation.



**Kexin Liu** received the M.Sc. degree in control science and engineering from Shandong University, Jinan, China, in 2013, and the Ph.D. degree in system theory from the Academy of Mathematics and Systems Science, Chinese Academy of Sciences, Beijing, China, in 2016. From 2016 to 2018, he was a Postdoctoral Fellow with Peking University, Beijing. He is currently an Associated Professor with the School of Automation Science and Electrical Engineering, Beihang University, Beijing. His current research interests include multi-agent systems and

complex networks.



**Lei Chen** received the Ph.D. degree in control theory and engineering from Southeast University, Nanjing, China, in 2018. He was a visiting Ph.D. student with the Royal Melbourne Institute of Technology University, Melbourne, VIC, Australia, and Okayama Prefectural University, Soja, Japan. From 2018 to 2020, he was a Postdoctoral Fellow with the School of Automation Science and Electrical Engineering, Beihang University, Beijing, China. He is currently with the Advanced Research Institute of Multidisciplinary Science, Beijing Institute of

Technology, Beijing, as an Associate Research Fellow. His current research interests include complex networks, characteristic model, spacecraft control, and network control.



**Jinhu Lü** (Fellow, IEEE) received the Ph.D. degree in applied mathematics from the Academy of Mathematics and Systems Science, Chinese Academy of Sciences, Beijing, China, in 2002. He was a Professor with RMIT University, Melbourne, VIC, Australia, and a Visiting Fellow with Princeton University, Princeton, NJ, USA. He is currently the Vice President of Beihang University, Beijing, China. He is also a Professor with the Academy of Mathematics and Systems Science, Chinese Academy of Sciences.

He is a Chief Scientist of the National Key Research and Development Program of China and a Leading Scientist of Innovative Research Groups of the National Natural Science Foundation of China. His current research interests include complex networks, industrial Internet, network dynamics, and cooperation control.

Prof. Lü was a recipient of the Prestigious Ho Leung Ho Lee Foundation Award in 2015, the National Innovation Competition Award in 2020, the State Natural Science Award three times from the Chinese Government in 2008, 2012, and 2016, respectively, the Australian Research Council Future Fellowships Award in 2009, the National Natural Science Fund for Distinguished Young Scholars Award, and the Highly Cited Researcher Award in engineering from 2014 to 2020. He is/was an Editor in various ranks for 15 SCI journals, including the Co-Editor-in-Chief of IEEE TRANSACTIONS ON INDUSTRIAL INFORMATICS. He served as a member in the Fellows Evaluating Committee of the IEEE CASS, the IEEE CIS, and the IEEE IES. He was the General Co-Chair of IECON 2017. He is a Fellow of CAA.